ACS Macro Letters

Letter

pubs.acs.org/macroletters

# Synthesis of Photoactuating Acrylic Thermoplastic Elastomers Containing Diblock Copolymer-Grafted Carbon Nanotubes

Markéta Ilčíková,[†,⊥] Miroslav Mrlík,[‡,⊥] Tomáš Sedláček,[‡] Miroslav Šlouf,[§] Alexander Zhigunov,[§] Kaloian Koynov,[∥] and Jaroslav Mosnáček*[,†]

[†]Polymer Institute, Slovak Academy of Sciences, Dúbravská cesta 9, 845 41, Bratislava, Slovakia

[‡]Centre of Polymer Systems, University Institute, Tomas Bata University in Zlin, Nad Ovcirnou 3685, 760 01 Zlin, Czech Republic

[§]Institute of Macromolecular Chemistry AS CR, Heyrovsky sq. 2, 16206 Prague 6, Czech Republic

[∥]Max Planck Institute for Polymer Research, Ackermanweg 10, D-55128 Mainz, Germany

Supporting Information

**ABSTRACT:** A photoactuating nanocomposite was prepared by the in situ grafting of carbon nanotubes with PBA-*b*-PMMA diblock copolymer during the synthesis of the linear triblock copolymer poly(methyl methacrylate)-*b*-poly(*n*-butyl acrylate)-*b*-poly(methyl methacrylate) (PMMA-*b*-PBA-*b*-PMMA). Control over the molecular characteristics of the block copolymers was achieved by applying atom transfer radical polymerization. This synthetic approach allowed for the excellent dispersion and distribution of carbon nanotubes within the polymer matrix. The final nanocomposite containing 1 wt % grafted carbon nanotubes exhibited improved elasticity compared to that of the pure triblock copolymer, as demonstrated by dynamic mechanical analysis and rotational rheology measurements. The photoactuating behavior of the nanocomposite was demonstrated by thermomechanical analysis.

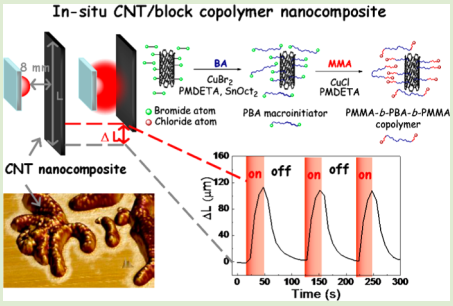


Acrylic block copolymers exhibit interesting properties that can be tuned by manipulating the structure and length of the blocks. The combination of polyacrylate soft block with polymethacrylate hard blocks in ABA triblock copolymers can provide materials with the properties of thermoplastic elastomers (TPEs). Compared to widely commercially used isoprene- or butadiene-containing TPEs, acrylic TPEs pose several advantages. Due to the absence of unsaturated bonds in the main chain, the acrylic-based block copolymers are more resistant to UV light.[1] In addition, versatile (meth)acrylic monomers allow for the service temperature to be tuned over a wide range of $T_g$, from approximately −50 to 200 °C.[2,3] Currently, reversible-deactivation radical polymerization (RDRP)[4a] (also called controlled/living[4b] and quasiliving[4c]) techniques are widely used for the preparation of block copolymers.[5−7] Among the different RDRP techniques that are available, atom transfer radical polymerization (ATRP) is considered the most versatile because it enables good control over the polymerization of acrylic, methacrylic, and styrene monomers.[8−10] ATRP has been successfully employed for the synthesis of a wide range of block copolymers with TPE properties.[11,12] In addition to linear block copolymers, block copolymers with star-like,[11−13] brush,[14] or branched[15] architectures have been synthesized. The properties of these copolymers differ from those of their linear analogues. For example, star-like copolymers exhibit better tensile strength and elongation at break than three-arm and linear copolymers with similar compositions.[11,12]

The incorporation of carbon nanotubes (CNTs) into a TPE matrix can lead to the improvement of certain material characteristics, such as electrical conductivity, mechanical properties, or photoactuation performance.[16−19] The dispersion and distribution of CNT in a polymer matrix remain key factors in the preparation of nanocomposites. It is well-known that CNTs tend to agglomerate into clusters that due to bad stress transfer from the matrix to the filler cause a deterioration of the final material's mechanical properties. In the case of photoactuating TPE nanocomposites in particular, the homogeneity of carbon dispersion is of great importance because inhomogeneous materials of this type suffer from an ineffective actuation response. In this respect, the in situ polymerization of the matrix in the presence of particles can lead to an improvement in the homogeneity of nanocomposites.[20]

Herein, the synthesis of new types of TPE nanocomposites consisting of linear triblock poly(methyl methacrylate)-*b*-poly(butyl acrylate)-*b*-poly(methyl methacrylate) copolymer (PMMA-*b*-PBA-*b*-PMMA) and brush diblock poly(butyl acrylate)-*b*-poly(methyl methacrylate) grafted onto the CNT surface (CNT-*g*-PBA-*b*-PMMA) is presented for the first time. The *in situ* approach of preparing the nanocomposites allowed for the excellent dispersion and distribution of CNTs within the matrix and an improvement in the viscoelastic properties of the

**Received:** July 23, 2014
**Accepted:** September 11, 2014
**Published:** September 15, 2014

  

final material compared to those of the pure matrix. The photoactuation ability of the final nanocomposite was demonstrated as well.

Nanocomposite synthesis was performed in two steps as shown in Scheme 1. First, *n*-butyl acrylate was polymerized in

**Scheme 1. Synthesis of the CNT-*g*-PBA-*b*-PMMA/PMMA-*b*-PBA-*b*-PMMA Nanocomposite**

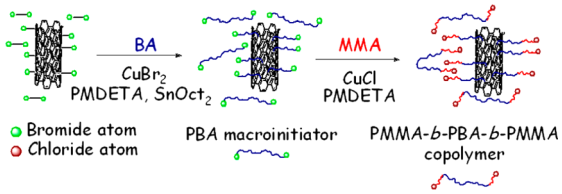


the presence of both a sacrificial difunctional ATRP initiator dimethyl 2,6-dibromoheptanedionate and CNT covalently premodified by an ATRP initiator in anisole. The free PBA chains and PBA chains covalently grafted onto the CNT surface were then extended with poly(methyl methacrylate) blocks.

The polymerization of PBA was performed using activator regenerated by electron transfer (ARGET) ATRP using $CuBr_2$/PMDETA as the catalytic system and $SnOct_2$ as a reducing agent. The polymerization was stopped at approximately 85% monomer conversion. The molar mass and dispersity of the PBA chains grown from the sacrificial initiator were approximately 65 000 g/mol and 1.3, respectively, as determined by gel permeation chromatography (GPC). On the basis of previous studies of "grafting from" polymerization techniques, the average molar mass of polymer chains attached to the CNT and that of chains grown from free low molecular weight initiator should be identical.[21] Accordingly, because we used a difunctional free initiator, the molar mass of the PBA chains grafted from the CNT could be expected to be 32 500 g/mol. In the following step, both the free and grafted PBA macroinitiators were chain extended by the ATRP of methyl methacrylate (MMA) using a CuCl/PMDETA catalytic system. The halide exchange technique was employed to facilitate the MMA polymerization in a controlled manner because the combination of a bromide macroinitiator with a CuCl catalyst ensures faster initiation compared to the propagation of MMA.[22,23] The MMA polymerization was stopped at 57% monomer conversion. The PBA:PMMA ratio in the final triblock copolymer, estimated by $^1$H NMR, was 100:33. The molar mass of the resulting copolymer PMMA-*b*-PBA-*b*-PMMA, calculated from the PBA:PMMA ratio, was 81 000 g/mol, taking into account a PBA molar mass of 65 600 g/mol. Accordingly, the molar mass of the PMMA blocks in both the free triblock copolymer and grafted diblock copolymer was 8000 g/mol. The dispersity of the triblock copolymer determined by GPC was 1.38, confirming that the polymerization was well controlled.

The CNT content in the final nanocomposite was determined by thermogravimetric analysis (TGA) and was observed to be approximately 1 wt %. Transmission electron microscopy confirmed the very good dispersion of CNT in the *in situ* prepared nanocomposite. As shown in Figure S1 (Supporting Information), CNTs were separated into individual nanotubes and homogeneously spread over the entire polymer matrix.

To analyze the grafted CNT, after both steps of the nanocomposite synthesis procedure, the grafted CNTs were separated from the polymer matrix via a combination of centrifugation and filtration from the nanocomposite solution. On the basis of TGA, the CNT-*g*-PBA contained an organic layer constituting approximately 40 wt % of its composition. Grafting density of the PBA chains on the CNT surface, calculated from TGA, molar mass of PBA chains, and specific surface area of CNT, was in the range of 0.02−0.3 PBA chains/nm$^2$. Taking into account the PBA:PMMA ratio in the block copolymer, the content of the grafted organic layer in CNT-*g*-PBA-*b*-PMMA was approximately 53 wt %.

The homopolymers and diblock copolymers on the CNT surfaces were visualized by scanning force microscopy (SFM).[24] The topography revealed nanotubes measuring 50−100 nm in height (Figure 1a, c). The corresponding phase contrast images

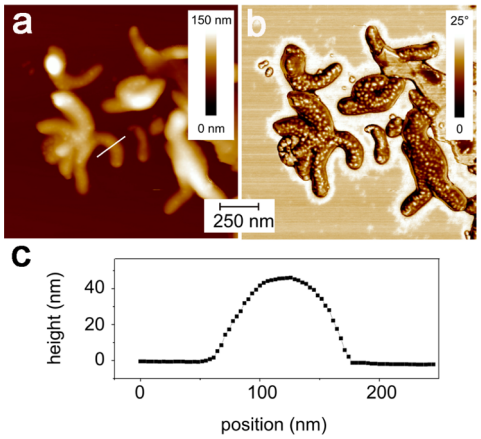


**Figure 1.** SFM images of CNT-*g*-PBA-*b*-PMMA in height (a) and phase (b) contrast; the height across the profile of the grafted nanotube (c).

showed a phase-separated morphology for the block copolymer grafted on the CNT surface (Figure 1b). Such phase-separated morphology was not observed on the samples prepared from CNT-*g*-PBA.

To investigate the impact of the grafted CNT on the morphology and properties of the matrix, the pure PMMA-*b*-PBA-*b*-PMMA copolymer matrix was separated from part of the final nanocomposite to obtain a reference polymer matrix with the same molecular characteristics as those of the matrix in the nanocomposite. The morphology was investigated using small-angle X-ray scattering (see Figure S2, Supporting Information). In the case of the pure matrix, PMMA blocks formed hexagonally packed cylinders. In contrast, the presence of CNTs, which were more than twice as thick as individual phases of the matrix, disrupted the regularity of the hexagonally packed cylinders. As shown in Figure S2 (Supporting Information), in the nanocomposite, the SAXS peaks were broader, and the supramolecular structure was less regular; as a result, the hexagonal symmetry could not be confirmed unambiguously based on SAXS.

The viscoelastic properties of both the nanocomposite and pure polymer matrix were studied by dynamic mechanical analysis (DMA) in shear mode. As shown in Figure 2, the presence of the CNT-*g*-PBA-*b*-PMMA enhanced both the storage and loss moduli of the PMMA-*b*-PBA-*b*-PMMA copolymer over the entire temperature range investigated.

In addition, as indicated by the inset in Figure 2, a shift in the glass transition temperature ($T_g$) of PBA to higher temper-


dx.doi.org/10.1021/mz500444m | *ACS Macro Lett.* 2014, 3, 999−1003

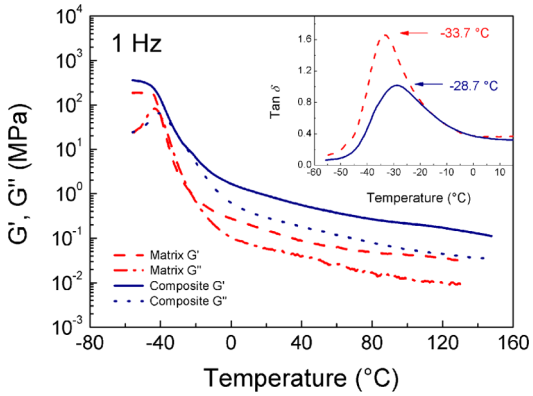


**Figure 2.** Temperature dependence of storage ($G'$) and loss moduli ($G''$) of pure PMMA-*b*-PBA-*b*-PMMA (matrix) and PMMA-*b*-PBA-*b*-PMMA containing 1 wt % CNT-*g*-PBA-*b*-PMMA (composite) measured at 1 Hz. Inset shows Tan $\delta$ as a function of temperature for both the matrix and nanocomposite.

atures was observed. On the basis of the structure of the CNT-*g*-PBA-*b*-PMMA, one can expect the involvement of the blocks of the grafted copolymer in the phase-separation process of the PMMA-*b*-PBA-*b*-PMMA matrix, leading to the preferential localization of the CNT in the soft PBA phase. Accordingly, the effect of the CNT on the $T_g$ of PBA toward the stiffening of the PBA phase, which was also observed, was expected.

To quantify the interactions of the grafted CNT with the polymer matrix, the activation energy ($E_a$) associated with the glass transition of the PBA phase was calculated according to a modified Arrhenius equation.[25] The values of $T_g$ for PBA as well as the corresponding $E_a$ are summarized in Table 1. The

**Table 1. Glass Transition Temperatures Determined at Various Frequencies and Calculated Activation Energies of Glass Transition of PBA Phases in the Pure PMMA-*b*-PBA-*b*-PMMA Matrix and PMMA-*b*-PBA-*b*-PMMA Containing 1 wt % CNT-*g*-PBA-*b*-PMMA**

| | $T_g$ of PBA phase (°C) | | | | |
|---|---|---|---|---|---|
| | 0.5 Hz | 1 Hz | 2.5 Hz | 5 Hz | $E_a$ (kJ/mol) |
| matrix | −35.5 | −33.7 | −31.3 | −29.5 | 184 |
| composite | −30.8 | −28.7 | −27.1 | −25.5 | 223 |

presence of CNT-*g*-PBA-*b*-PMMA in the polymer matrix resulted in the enhancement of $E_a$ for the glass transition of PBA by 39 kJ/mol, which corresponds to a 21% increase. In other words, in the presence of 1 wt % of the grafted CNT the polymer chains needed more energy to induce the transition, which is indicative of the good interactions between CNT-*g*-PBA-*b*-PMMA and the PBA chains of the PMMA-*b*-PBA-*b*-PMMA matrix.

The viscoelastic properties of the matrix and nanocomposite at elevated temperatures were investigated using rotational rheology in oscillatory shear mode. Figure 3 shows the frequency dependence of the storage and loss moduli at 200, 240, and 260 °C for both the nanocomposite and pure polymer matrix. At 200 °C, the $G'$ and $G''$ values of the matrix and nanocomposite exhibited a linear frequency dependence; the storage modulus dominated over the loss modulus over the entire frequency range tested, indicating the solid-like behavior of both materials. The values of $G'$ and $G''$ were higher in the nanocomposite material due to the restriction of polymer chain

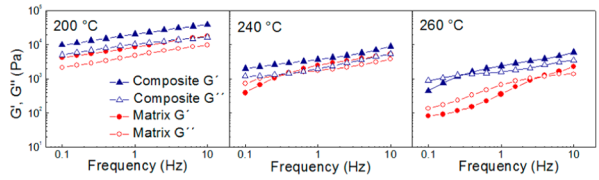


**Figure 3.** Frequency dependence of storage ($G'$) and loss modulus ($G''$) of 1 wt % CNT-*g*-PBA-*b*-PMMA/PMMA-*b*-PBA-*b*-PMMA (composite) and PMMA-*b*-PBA-*b*-PMMA (matrix) at 200, 240, and 260 °C.

motion and the interactions between the polymer chains and grafted CNT.

A more pronounced effect of CNT-*g*-PBA-*b*-PMMA on the rheological behavior of the matrix was observed at 240 °C, at which a cross-point of the $G'$ and $G''$ values of the matrix was observed at 0.3 Hz. Thus, at frequencies below 0.3 Hz, the liquid-like behavior of the matrix dominates over the solid-like behavior. In contrast, in the nanocomposite, the solid-like behavior was retained over the entire frequency range tested. The nanocomposite's $G'$ and $G''$ cross-point was observed to occur at 260 °C at 0.2 Hz. On the other hand, at 260 °C the pure polymer matrix exhibited liquid-like behavior over nearly the entire frequency range tested.

Finally, the photoactuation ability of both the matrix and nanocomposite was investigated. Actuation describes a material's ability to undergo reversible shape changes in response to an external stimulus.[26] In the case of the photoactuation of CNT-based polymer nanocomposites, the preoriented CNTs absorb incident light and transform the light energy to heat. The heat is transferred to prestained and oriented polymer chains in the vicinity of the CNT, and hence, the actuation performance of the polymeric material is significantly enhanced.[16,27] In our preceding studies the various TPEs were used such as ethylene-vinylacetate (EVA) elastomer[17] or poly(styrene-*b*-isoprene-*b*-styrene) (SIS) block copolymer.[16] It was observed that composites containing CNT and EVA elastomer exhibit loss of elasticity during photo-actuation due to local overheating. On the other hand, in SIS block copolymer TPE the present CNT interacted with the polystyrene phase, resulting in disturbing the physical cross-linking and giving nonstable photoactuation behavior. There were also studies utilizing TPU elastomer and modified graphene;[28] however, these materials needed high values of prestrain to obtain the contraction after irradiation. A similar phenomenon was also observed in cross-linked PDMS-based graphene composites[29] as is discussed below. A further drawback of chemically cross-linked elastomers is the impossibility of their reprocessability. Therefore, in this study, the photoactuation ability of the synthesized TPE based on PMMA-*b*-PBA-*b*-PMMA triblock copolymer and its composite with CNTs was investigated for the first time. Also this is a pioneer study in utilization of the thermomechanical analysis (TMA) for photoactuation investigation at room temperature.

Nanocomposite strips were fixed in TMA clamps and loaded with a force of 0.05 N to prestretch the PBA chains along one direction, and the samples were irradiated by a red laser diode for either 10 or 30 s. As expected, contraction of the samples during irradiation was observed. Figure 4 shows the changes in sample length, $\Delta L$, that occurred during irradiation.

As expected, the range of contraction increased with increasing light power. Unlike the nanocomposite, either the


dx.doi.org/10.1021/mz500444m | ACS Macro Lett. 2014, 3, 999−1003

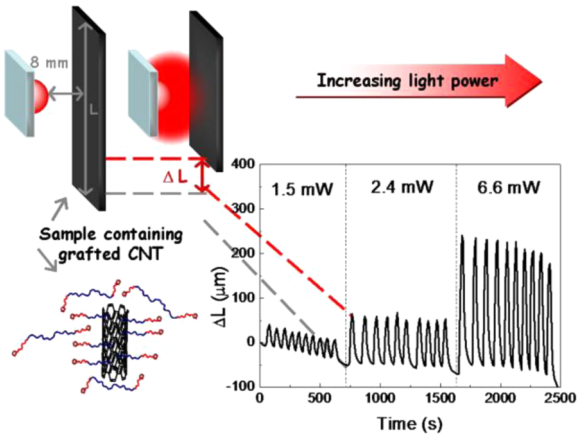


**Figure 4.** Investigation of photoactuation ability by TMA. Monitoring of nanocomposite actuation length contraction, $\Delta L$, when samples were irradiated under a preload of 0.05 N for 30 s at various diode powers: 1.5, 2.4, and 6.6 mW.

pure matrix was unable to exhibit any actuation at the lowest investigated power (1.5 mW) or a contraction that was lower by more than 1 order of magnitude was observed when higher light powers were applied (see Figure S3, Supporting Information). In the case of the nanocomposite, the highest actuation contractions at red laser diode powers of 6.6 and 18.5 mW reached 278 ± 16 and 398 ± 16 $\mu$m, respectively. These values correspond to length changes of 3.2% and 4.5%, respectively, calculated as $(L_0 - L)/L_0$, where $L_0$ and $L$ are the lengths of the nonirradiated and irradiated sample, respectively. For comparison, a recent study on the photoactuation of a 2 wt % graphene/polydimethylsiloxane composite tested under similar conditions with a light power of 6.8 mW showed a maximum contraction of 2.3%. In that case, however, much higher prestrain (40% compared with the 7.4% used in this study) was needed, whereas no contraction was observed at prestrain levels of up to 10%.[30] Thus, the preliminary results suggest that the synthesized nanocomposite material exhibits great potential for sensing applications. More in-depth photoactuation studies of acrylic TPE nanocomposites are currently underway.

In summary, the synthesis of acrylic TPEs by the growth of the PBA-*b*-PMMA diblock copolymer from CNT surfaces in the same steps during the synthesis of a PMMA-*b*-PBA-*b*-PMMA triblock copolymer matrix was described for the first time. The final nanocomposites, containing only 1 wt % of well-dispersed, compatibilized CNT, showed a significant improvement in viscoelastic performance over a wide temperature range compared to that of the pure copolymer matrix. Finally, it was proved that the CNT-*g*-PBA-*b*-PMMA/PMMA-*b*-PBA-*b*-PMMA nanocomposite is a promising photoactuating material with a fast and reversible response to red light.

## ■ ASSOCIATED CONTENT

### Supporting Information

Experimental details, TEM image of nanocomposite, SAXS analysis, and photoactuation measurements. This material is available free of charge via the Internet at http://pubs.acs.org.

## ■ AUTHOR INFORMATION

### Corresponding Author

*E-mail: jaroslav.mosnacek@savba.sk. Phone: +421 2 3229 4353.

### Present Address

[⊥]Centre for Advanced Materials, P.O. Box 2713, Doha, Qatar.

### Author Contributions

The manuscript was written with contributions from all authors.

### Notes

The authors declare no competing financial interest.

## ■ ACKNOWLEDGMENTS

The authors thank the Slovak Research and Development Agency APVV through Grant APVV-0109-10, Centre of Excellence SAS for Functionalized Multiphase Materials (FUN-MAT), the European Commission within seventh Frame Program (project NOMS, contract no. 228916), and DAAD project 50755038 "Fluorescent labels for optimization of graphene distribution in graphene/polymer nano-composite materials with improved properties". MM and TS also thank the Operational Program Research and Development for Innovations cofunded by the European Regional Development Fund and national budget of Czech Republic, within the framework of project Centre of Polymer Systems (CZ.1.05/2.1.00/03.0111) for their support. Electron microscopy was performed with financial support provided through grant TACR TE01020118. Furthermore, the authors thank Rüdiger Berger and Uwe Rietzler for analyzing our samples by scanning force microscopy.

## ■ REFERENCES

(1) Holden, G.; Bishop, E. T.; Legge, N. R. *J. Polym. Sci. C* **1969**, 37–57.
(2) Yu, J. M.; Dubois, P.; Jerome, R. *Macromolecules* **1996**, *29*, 8362–8370.
(3) Yu, J. M.; Dubois, P.; Jerome, R. *Macromolecules* **1996**, *29*, 7316–7322.
(4) (a) Jenkins, A. D.; Jones, R. G.; Moad, G. *Pure Appl. Chem.* **2010**, *82*, 483–491. (b) di Lena, F.; Matyjaszewski, K. *Prog. Polym. Sci.* **2010**, *35*, 959–1021. (c) Szanka, A.; Szarka, G.; Ivan, B. J. *Macromol. Sci., Pure Appl. Chem.* **2014**, *51*, 125–133.
(5) Keddie, D. J. *Chem. Soc. Rev.* **2014**, *43*, 496–505.
(6) Ran, J.; Wu, L.; Zhang, Z.; Xu, T. *Prog. Polym. Sci.* **2014**, *39*, 124–144.
(7) Davis, K. A.; Matyjaszewski, K. *Adv. Polym. Sci.* **2002**, *159*, 1–169.
(8) Grimaud, T.; Matyjaszewski, K. *Macromolecules* **1997**, *30*, 2216–2218.
(9) Matyjaszewski, K.; Patten, T. E.; Xia, J. H. *J. Am. Chem. Soc.* **1997**, *119*, 674–680.
(10) Matyjaszewski, K.; Shipp, D. A.; Wang, J. L.; Grimaud, T.; Patten, T. E. *Macromolecules* **1998**, *31*, 6836–6840.
(11) Nese, A.; Mosnacek, J.; Juhari, A.; Yoon, J. A.; Koynov, K.; Kowalewski, T.; Matyjaszewski, K. *Macromolecules* **2010**, *43*, 1227–1235.
(12) Juhari, A.; Mosnacek, J.; Yoon, J. A.; Nese, A.; Koynov, K.; Kowalewski, T.; Matyjaszewski, K. *Polymer* **2010**, *51*, 4806–4813.
(13) Kuckling, D.; Wycisk, A. *J. Polym. Sci., Polym. Chem.* **2013**, *51*, 2980–2994.
(14) Sheiko, S. S.; Sumerlin, B. S.; Matyjaszewski, K. *Prog. Polym. Sci.* **2008**, *33*, 759–785.
(15) Gao, C.; Yan, D. *Prog. Polym. Sci.* **2004**, *29*, 183–275.
(16) Ilčíková, M.; Mrlík, M.; Sedláček, T.; Chorvát, D.; Krupa, I.; Šlouf, M.; Koynov, K.; Mosnáček, J. *Polymer* **2013**, *55*, 211–218.
(17) Czaniková, K.; Ilčíková, M.; Krupa, I.; Mičušík, M.; Kasák, P.; Pavlova, E.; Mosnáček, J.; Chorvát, D., Jr.; Omastová, M. *Smart Mater. Struct.* **2013**, *22*, 104001.
(18) Koerner, H.; Price, G.; Pearce, N. A.; Alexander, M.; Vaia, R. A. *Nat. Mater.* **2004**, *3*, 115–120.

(19) Liang, J.; Xu, Y.; Huang, Y.; Zhang, L.; Wang, Y.; Ma, Y.; Li, F.; Guo, T.; Chen, Y. *J. Phys. Chem. C* **2009**, *113*, 9921−9927.
(20) Fukushima, T.; Kosaka, A.; Yamamoto, Y.; Aimiya, T.; Notazawa, S.; Takigawa, T.; Inabe, T.; Aida, T. *Small* **2006**, *2*, 554−560.
(21) Yoon, J. T.; Lee, S. C.; Jeong, Y. G. *Compos. Sci. Technol.* **2010**, *70*, 776−782.
(22) Matyjaszewski, K.; Shipp, D. A.; Wang, J.-L.; Grimaud, T.; Patten, T. E. *Macromolecules* **1998**, *31*, 6836−6840.
(23) Mosnáček, J.; Matyjaszewski, K. *Macromolecules* **2008**, *41*, 5509−5511.
(24) Butt, H. J.; Berger, R.; Bonaccurso, E.; Chen, Y.; Wang, J. *Adv. Colloid Interface Sci.* **2007**, *133*, 91−104.
(25) Geethamma, V. G.; Kalaprasad, G.; Groeninckx, G. l.; Thomas, S. *Composites, Part A* **2005**, *36*, 1499−1506.
(26) Lendlein, A.; Kelch, S. *Angew. Chem., Int. Ed.* **2002**, *41*, 2034−2057.
(27) Ahir, S. V.; Terentjev, E. M. *Nat. Mater.* **2005**, *4*, 491−495.
(28) Liang, J. J.; Xu, Y. F.; Huang, Y.; Zhang, L.; Wang, Y.; Ma, Y. F.; Li, F. F.; Guo, T. Y.; Chen, Y. S. *J. Phys. Chem. C* **2009**, *113*, 9921−9927.
(29) Zhao, Y.; Song, L.; Zhang, Z.; Qu, L. *Energy Environ. Sci.* **2013**, *6*, 3520−3536.
(30) Loomis, J.; King, B.; Burkhead, T.; Xu, P.; Bessler, N.; Terentjev, E.; Panchapakesan, B. *Nanotechnology* **2012**, *23*, 045501.